Influence of decreasing temperature on aerobic granular sludge - microbial community dynamics and treatment performance

Bioresource Technology Reports 25 (2024) 101792

Contents lists available at ScienceDirect

Bioresource Technology Reports

journal homepage: www.sciencedirect.com/journal/bioresource-technology-reports

Influence of decreasing temperature on aerobic granular sludge - microbial community dynamics and treatment performance

Jennifer Ekholm [a], Cecilia Burzio [a], Amir Saeid Mohammadi [a], Oskar Modin [a], Frank Persson [a], David J.I. Gustavsson [b,c], Mark de Blois [d], Britt-Marie Wilén [a,*]

[a] Division of Water Environment Technology, Department of Architecture and Civil Engineering, Chalmers University of Technology, SE-41296 Gothenburg, Sweden
[b] Sweden Water Research AB, Ideon Science Park, Scheelevägen 15, SE-22370 Lund, Sweden
[c] VA SYD, P.O. Box 191, SE-20121 Malmö, Sweden
[d] H2OLAND, Grindgatan 1, SE-44136 Alingsås, Sweden

ARTICLE INFO

Keywords:
Aerobic granular sludge
Municipal wastewater treatment
Nitrogen and phosphorus removal
Decreasing temperatures
Fluctuating conditions

ABSTRACT

Municipal wastewater in temperate climates is characterized by seasonal temperature changes. Temperature is a determining factor for biological processes, but the impact of gradually decreasing temperature on aerobic granular sludge (AGS) has been largely unexplored. In this study, the influence of decreasing temperature from 20 °C to 6 °C on AGS was investigated at rates of 0.5 and 1 °C per week. Temperature was a major driver for microbial community change, where the community response could be divided into three main subclusters. Strains within the guilds of ammonium- and nitrite-oxidising bacteria (AOB and NOB) as well as polyphosphate- and glycogen-accumulating organisms (PAOs and GAOs) grouped in different subclusters, indicating variable responses among and between the guilds. The phosphorous removal rate was sufficient for complete removal at all temperatures, presumably due to functional redundancy within the PAOs. The nitrification rate was, however, seriously impaired below 13 °C, despite diversity within AOB and NOB.

1. Introduction

Aerobic granular sludge (AGS) is an emerging wastewater treatment technology with increasing full-scale applications worldwide (Hamza et al., 2022). AGS is a special type of biofilm where the microorganisms grow in dense aggregates with excellent settling properties, high biomass retention and capability to remove organic matter, nitrogen, and phosphorus in a single reactor, which enable small land footprint and energy-efficient operation (Pronk et al., 2015). The reactor conditions applied in AGS operation select for a microbial community with high abundances of functional groups of microorganisms (Ali et al., 2019), such as polyphosphate accumulating organisms (PAOs), glycogen accumulating organisms (GAOs), nitrifiers, and denitrifiers. Organic matter is taken up and stored intracellularly by PAOs, and GAOs during the anaerobic feeding (de Kreuk and van Loosdrecht, 2004). Residual organic matter is removed in the aerobic/anoxic phase by aerobic heterotrophs and denitrifiers. PAOs accumulate phosphorus in the form of polyphosphate, which is removed with the sludge withdrawal. The phosphorus removal depends on the competition between PAOs and GAOs for the available organic carbon substrate (Weissbrodt et al., 2013). Due to the dense structure of the granular biomass, only diffusible substrate such as volatile fatty acids (VFAs) will be available inside the granule (Layer et al., 2019). Non-diffusible substrates can be hydrolysed on the granule surface or by the floccular fraction of biomass often present in AGS systems (Ekholm et al., 2022; Layer et al., 2019; Toja Ortega et al., 2021a). Nitrogen is removed in several steps via nitrification by ammonia-oxidising bacteria (AOB), nitrite-oxidising bacteria (NOB), and bacteria capable of complete ammonium oxidation (comammox). The nitrifiers are slow-growing and known to be temperature-sensitive. The nitrogen is further converted into nitrogen gas by denitrifiers. The denitrification process consists of four enzymatic reactions. Some bacteria have the genes for all reactions, but many denitrifiers have just one or a few of the genes (Gao et al., 2019).

Temperature is a crucial parameter affecting microbial metabolism and temperature variation plays a key role in microbial community dynamics (Adams et al., 2010). In AGS, operational problems such as washout of biomass, disintegration of granules, worsening settling properties, and deteriorating nutrient removal have been correlated

* Corresponding author.
E-mail address: britt-marie.wilen@chalmers.se (B.-M. Wilén).

https://doi.org/10.1016/j.biteb.2024.101792
Received 30 November 2023; Received in revised form 13 February 2024; Accepted 16 February 2024
Available online 17 February 2024

with low temperatures in lab-scale studies (Gonzalez-Martinez et al., 2018; Winkler et al., 2012). A recent full-scale study concluded that the AGS performance was highly influenced by the local conditions, including low temperatures during the winter season (Ekholm et al., 2022). The majority of the recent lab-scale studies of temperature influence on AGS have focused on constant temperatures (Bassin et al., 2012; Gonzalez-Martinez et al., 2018; Gonzalez-Martinez et al., 2017; Muñoz-Palazon et al., 2018; Muñoz-Palazon et al., 2020a; Muñoz-Palazon et al., 2020b; Muñoz-Palazon et al., 2022; Wang et al., 2020; Winkler et al., 2012), showing impact on the granule stability, microbial community composition, and nutrient removal performances. However, in climate regions with seasonal temperature dynamics, the full-scale reactor temperature continuously changes over time (Ekholm et al., 2022). Influence of temperature decrease was previously studied in different wastewater treatment systems (Liu et al., 2022b; Wang et al., 2018), but AGS systems are relatively unexplored (Zhou et al., 2018). Previously, the nitrification was shown to be sensitive to decreasing temperature (26–13 °C) in halophilic AGS treating high-salinity synthetic wastewater (Han et al., 2022). At geographical regions with large seasonal temperature dynamics, it is essential to assess limitations of the functional performance of AGS processes operated at low and decreasing temperatures. Hence, further attention to AGS under low and decreasing temperatures is needed (Zhou et al., 2018).

The abundance and performances of functional groups of PAOs, GAOs, AOB, NOB, and denitrifiers are interlinked, and a temperature decrease might shift the balance of cooperation and competition, as they are likely influenced by temperature to varying extent. The responses of different microbial genera depend on their optimal temperature for growth. The microorganisms grow more slowly outside their optimal temperature, but can adapt to their local environment, for example cold-adapted AOB and NOB were previously reported in several studies (Alawi et al., 2007; Kruglova et al., 2020). Furthermore, the temperature influences the microbial community as a whole, with lower temperatures leading to lower diversity (Muñoz-Palazon et al., 2022), which might decrease the functional redundancy and thereby the stability of the reactor functions (Leventhal et al., 2018).

This study aims at increasing the understanding of how decreasing temperature affects the granule structure, microbial composition and diversity, and how this in turn affects the function of the AGS process. Two lab-scale AGS sequencing batch reactors (SBRs) were run with two different rates of temperature decrease, which were close to actual rates of temperature decrease that can be observed in municipal wastewater in temperate climates.

2. Materials and methods

2.1. Experimental set-up

2.1.1. Reactor and cycle design

Aerobic granular sludge was cultivated in two parallel sequencing batch reactors (SBRs) made of glass with an operating volume of 3.2 L, inner diameter of 5.6 cm and height of 160 cm, equipped with double walls connected to cooling water baths for temperature control. The pH value was controlled at 7.5 ± 0.3 by adding 1 M NaOH and 1 M HCl. The cycle phases (Table S2), hydraulic retention time (12*h*) and the volume exchange (50 %) were fixed. The reactors were operated at a solids retention time of approximately 30 days. The dissolved oxygen (DO) concentration was controlled for the whole experiment at 20 % ± 10 % saturation resulting in 2.2 ± 1.1 mg DO L^{-1} during the aeration phase. Gas was supplied at the bottom of the reactor through a gas diffuser at a flow rate of 5 L min^{-1}. This corresponds to hydrodynamic shear forces of 0.211, 0.219, 0.225, 0.231, 0.244, and 0.254 [Nm^{-2}], at 20, 17, 15, 13, 9 and 6 °C, respectively (Arrojo et al., 2008; Yan et al., 2020) (as detailed in supplementary information, Table S1). The DO level was controlled by a gas recirculation system. If the measured DO value was deviated by more than ±10 % from the DO setpoint, air or nitrogen gas was added using mass flow controllers.

2.1.2. Influent media composition

The composition of the synthetic wastewater contained multiple organic carbon sources, recipe adaption from Layer et al. (2019), consisted of equal concentrations (as COD equivalents) of acetate, propionate, glucose, and peptone from enzymatic digest (Table 1). The carbon sources and ammonium nitrogen (NH_4Cl) were mixed in one media bottle, together with the salts $CaCl_2$, $MgSO_4$ and KCl. Alkalinity ($NaHCO_3$) and micronutrient solution were added to the phosphorus media (KH_2PO_4 and K_2HPO_4). The influent concentrations were 400 mg L^{-1} COD, 50 mg L^{-1} nitrogen and 6 mg L^{-1} phosphate phosphorus. The micronutrient solution composition is provided in the supplementary material (Table S3).

2.1.3. Start-up and sampling

Mature granules from the Nereda® process at the wastewater treatment plant (WWTP) in Strömstad, Sweden, performing enhanced biological nitrogen- and phosphorus removal (Ekholm et al., 2022) was used as inoculum to the reactors. Before inoculation, the granules were sieved (1 mm pore size) and added at a concentration of approximately 7 g L^{-1} (Fig. 1). During start-up, the settling time was gradually decreased from 90 to 3 min over a period of 50 days. The process performance was investigated by sampling the reactor content at the start of the aeration phase (after 1 min of aeration to get a representative sample) and the effluent, twice per week. Cycle studies were performed at temperatures of 20, 17, 15, 9 and 6 °C in triplicate to assess the specific nitrification rates and phosphorus uptake rates.

2.1.4. Temperature alteration rate

The temperature was lowered to mimic the seasonal shift from warmer to colder temperatures and to study the influence of the rate of this shift. Typical temperature decrease rates of approximately 0.4 and 0.5 °C per week, have been observed at WWTPs in the south/south-west of Sweden (Table S4). Faster temperature decreasing rates have also been observed (Arnell et al., 2021; la Cour Jansen et al., 1992). In this study, two temperature decrease rates were investigated: 0.5 °C (R2) and 1 °C (R1) per week. The faster decrease rate was applied to amplify the influence of decreasing temperature, and to study the influence of lower temperatures (6–12 °C). Winter wastewater temperatures down to 6 °C is common in the southern parts of Sweden in the coldest period. Except for the temperature during the experimental period, all other operational parameters were kept the same between the two reactors.

2.2. Microbial community analysis

The composition and dynamics of the microbial community was analysed by amplicon sequencing of the 16S rRNA gene. The biomass samples were collected from the middle and bottom ports of the reactor, combined, mixed with a blender, and immediately stored at −20 °C. The

Table 1
Influent media composition.

Compound	Formula	Influent concentration (mg L^{-1})
Sodium acetate	$NaC_2H_3O_2$	128
Sodium propionate	$C_3H_5NaO_2$	80
Glucose	$C_6H_{12}O_6$	94
Peptone from meat, enzymatic digest	$C_2H_3N_3$	81
Ammonium chloride	NH_4Cl	144
Calcium dichloride	$CaCl_2{\cdot}H_2O$	18
Magnesium sulphate	$MgSO_4$	16
Potassium chloride	KCl	33
Potassium dihydrogen phosphate	KH_2PO_4	13
di-Potassium hydrogen phosphate	K_2HPO_4	1
Sodium bicarbonate	$NaHCO_3$	200

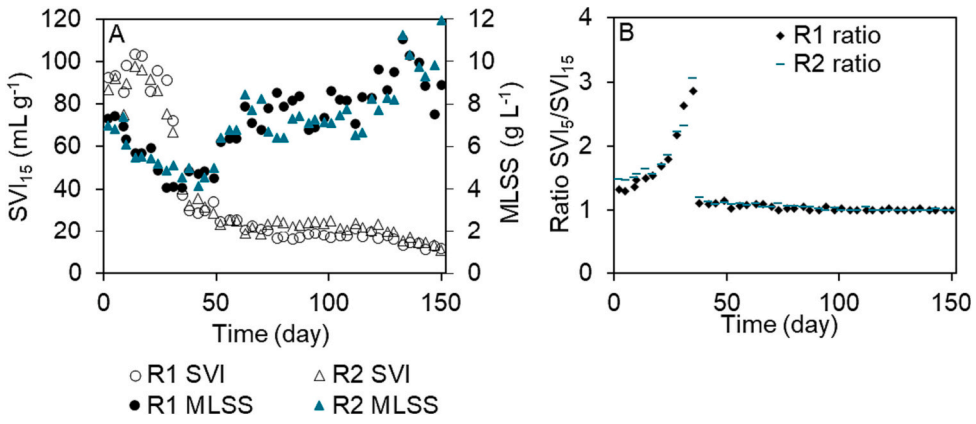

Fig. 1. A) MLSS concentration and sludge volume index after 15 min, B) ratio of sludge volume index after 5 and 15 min.

workflow follows the procedures described in Ekholm et al. (2022). Briefly, DNA was extracted from 15 mL of homogenized sludge using the FastDNA spin kit for soil. The V4 region of the 16S rRNA gene was amplified by PCR using indexed primers. The PCR products were purified and pooled prior to sequencing using a MiSeq, reagent kit V3. Sequence processing and generation of consensus count tables of amplicon sequence variants (ASVs) was conducted using DADA2 (Callahan et al., 2016) and VSEARCH (Rognes et al., 2016) in parallel according to Modin et al. (2020), using Midas 4.8.1 for taxonomy (Dueholm et al., 2022). Raw sequence reads are deposited at the NCBI sequence read archives (SRA) accession PRJNA952915.

2.3. Water and sludge analysis

The water samples were filtered through 0.2 μm pore size filters prior to the analysis of nitrogen species (NH_4^+-N, NO_3^--N, NO_2^--N), PO_4^{3-}-P, dissolved organic carbon (DOC) and total nitrogen (TN). The suspended solids, mixed liquor suspended solids (MLSS), and volatile suspended solids (VSS) were analysed by standard methods (APHA, 2005). The sludge volume index after 5, 10 and 15 min (SVI_5, SVI_{10} and SVI_{15}) was determined in situ from the bed volume of settled biomass.

Eq. (1) was used to estimate the solids retention time (SRT):

$$SRT = \frac{V \bullet X}{Q_{ex} \bullet X_{ex} + Q_{eff} \bullet X_{eff}} \quad (1)$$

V is the reactor volume (L), X is the MLSS concentration in the reactor (g L^{-1}), Q_{ex} is the average flow rate of excess sludge over a week (L d^{-1}), X_{ex} is the MLSS concentration of the excess sludge (g L^{-1}), Q_{eff} is the flow rate of effluent (L d^{-1}), and X_{eff} is the SS concentration in the effluent (g L^{-1}). The excess sludge was purged from the bottom port (50 %) and the effluent port (50 %) at the end of the aeration phase. The SRT was controlled at roughly 30 days by the removal of excess sludge.

Granule sizes were estimated by taking 50 images (Nikon CoolpixA900) of granules diluted in tap water to avoid overlapping aggregates. Photos were calibrated with known distance and processed by ImageJ software (https://imagej.nih.gov/ij) by calculating the area of granules from binary images. The granules were almost spherical, and their diameter (D_0) can be approximated from the projected area (A) as:

$$D_0 = 2\sqrt{\frac{A}{\pi}} \quad (2)$$

2.4. Data analysis

The water and sludge data were analysed with linear regression, *t*-test for paired samples and correlation tests (Pearson), using statistical tools in the excel-add-in package Real Statistics. *P*-values below 0.05 were considered significant.

Diversity indices, principal coordinates analysis (PCoA) and heatmaps were produced in qdiv (Modin et al., 2020). Within-sample (alpha) diversity (^qD) and dissimilarity (^qd) between samples (Chao et al., 2014) were measured using the Hill number framework in which the diversity order q represents the weight of the relative abundance of taxa (Jost, 2006). The ASVs are given equal weight, irrespective of their relative abundances at $q = 0$ and the alpha diversity is then identical to the richness, i.e., the number of ASVs detected. At $q = 1$, the ASVs are weighted according to their relative abundance, meaning that for alpha diversity and dissimilarity, the 'common'ASVs are emphasised. At $q = 2$, ASVs with high relative abundance are emphasised.

Network analysis was carried out to identify co-occurrence patterns between ASVs in the microbial community. In the network analysis, ASVs detected in at least 50 % of the samples were included. The correlation matrix was determined using fastspar v1.0.0 (Watts et al., 2018), which is an implementation of the SparCC algorithm (Friedman and Alm, 2012). Correlations with a *p*-value below 0.05 and a correlation coefficient above 0.8 were retained. NetworkX v2.8.4 was used to visualize the network and infer sub-communities (Hagberg et al., 2008).

3. Results

3.1. Granule characteristics

The biomass in the SBRs was first adapted to the new operational- and environmental conditions. After approximately 40 days, the SVI_{15} had drastically decreased to <40 mL g^{-1} (Fig. 1A). Also, the ratio between SVI after 5 and 15 min dropped to 1, indicating well granulated biomass with fast settling, which remained until the end of the experiment (Fig. 1B). During the adaptation period, the morphology of the granules was shifting from a mixture of dark small granules and floccular sludge in the inoculum to larger granules in both reactors (Fig. S1). From day 54 the temperature was decreased weekly by 1 °C and 0.5 °C in R1 and R2, respectively. The MLSS concentrations first decreased, and later increased from around 4 g L^{-1} (day 40) to around 10 g L^{-1} at the end of the study. The sludge production over the whole study period was estimated to 0.6 g MLSS d^{-1} in both reactors. The average granule diameter was similar between the reactors ($p > 0.05$), and the granular morphology and size did not seem to be influenced by the temperature (Fig. S1A). Assuming the granules are spherical, the volume-based size distribution indicated a median size ranging from 1.8 to 3.8 mm for R1 and 0.2–4.5 mm for R2. The average diameter in R2 increased over time. In contrast, for R1, the average diameter increased until day 128 (when 9 °C was reached) before diminishing (Fig. S1B and C). The ratio of VSS to MLSS was stable at 85–90 % in both reactors from start-up until the end of the study. The effluent concentrations of suspended solids varied and were 0.06 ± 0.03 and 0.05 ± 0.02 g L^{-1} for R1 and R2, respectively, and had no correlation with the temperature ($p > 0.05$).

3.2. Impacts of altering temperature on nutrient removal

3.2.1. Removal of organic matter and phosphorus

The total removal of organic matter was steady in both reactors at all temperatures: 96 ± 3 % for R1 and 96 ± 2 % for R2, corresponding to an average effluent concentration of 16 ± 7 mg DOC L^{-1} in both reactors. During the adaptation period, relatively more of the DOC was removed in the aeration phase (23–31 %), than after day 50 when less was removed in the aeration (9–11 %), and most of the DOC was taken up in the anaerobic feeding phase. However, towards the end of the study, the DOC uptake in the feeding phase was reduced (Fig. S2). The concentrations of DOC removed during feeding were similar in both reactors and were correlated with the temperature during the temperature decrease period ($p < 0.05$). The anaerobic uptake rate of organic matter ranged from approximately 6 to 14 mg DOC g VSS^{-1} h^{-1} (rate based on 90 min of feeding) and the concentrations of released phosphate ranged from around 25 to 40 mg P L^{-1} (Fig. S2). The removal of phosphate was 99 ± 3 % for both reactors during the whole experiment (Fig. 2) with effluent concentrations of 0.3 ± 1.1 and 0.2 ± 0.6 mg L^{-1} in R1 and R2, respectively.

3.2.2. Removal of nitrogen

The effluent concentrations of ammonium were under the detection limit in both reactors during the adaptation period (with a few exceptions) and the following first weeks of the temperature decrease period. The nitrification capacity started to deteriorate when each reactor had reached around 15 °C, seen as increasing concentrations of ammonium in the effluent (Fig. 2). However, nitrite did not accumulate considerably and the effluent concentrations of nitrite were generally low throughout the experimental run, whereas the nitrate concentrations decreased in both reactors. The concentrations of total nitrogen in the effluent were decreasing until around 15 °C in both reactors (Fig. S2). The decreasing nitrate concentrations was due to higher total removal of nitrogen down to 16 °C and 15 °C in R1 and R2, respectively, whereafter the ammonium effluent concentrations increased and hence the removal of total nitrogen decreased. Around day 45, an elevated effluent concentration of ammonium was observed in R1, but no particular reason for this event was identified.

3.3. In-situ conversion rates

Cycle studies were performed at 20, 17, 15, 13, 9, and 6 °C to evaluate the reactor concentration profiles under the aeration phase (Fig. S3). Specific nitrification and P-uptake- and DOC oxidation rates were calculated based on the cycle studies. There were significant correlations between temperature and specific nitrification rates ($p < 0.05$) with slightly higher rates at 15 °C in R2 compared to in R1 (Fig. 3). In contrast, at 13 °C the nitrification was completely lost in R2, but not in R1. The specific P-uptake rate in R1 was significantly correlated with temperature ($p < 0.05$). In R2 the P-uptake rates were similar for temperatures between15–20 °C (approximately 3.5 mg P g VSS^{-1} h^{-1}) but slowed down at 13 °C to 1.5 mg P g VSS^{-1} h^{-1} (Fig. 3). A significant correlation between removal rate of DOC (mg DOC g VSS^{-1} h^{-1}) and decreasing temperature was observed in R1 ($p < 0.05$) but not in R2. However, the association between temperature and DOC removal rates was similar in both reactors and the lack of statistically significant correlation in R2 was likely due to the smaller temperature range. The *p*-values for the correlations between specific conversion rates and temperature are presented in Table S5.

3.4. Microbial community succession

The alpha diversity at both q = 0 and q = 1 was decreasing with time at a similar rate in R1 and R2, starting before the temperature decrease was initiated (Fig. 4A). However, the diversity was lower in R1 than R2 after 100 days, when the temperature in R1 and R2 was 13 °C and 16.5 °C, respectively. The alpha diversity for q = 2 and the evenness (q = 1, Pielou) also decreased over time in both reactors, but with lower values for R1 at temperatures below 13 °C (Fig. S4). During the temperature decrease, the diversity (q = 0 and q = 1) was lower in R2 compared to R1 when exposed to the same temperature (Fig. S5).

Ordination using principal coordinate analysis (q = 1) showed that the microbial communities in the two reactors had a similar succession and diverged from each other when the temperature decrease had started (Fig. 4B). The dissimilarity of each sample compared with the seed was increasing over time with larger dissimilarities at q = 1 than q = 0 (Fig. S6A). However, the rate of change, that is the dissimilarity between two consecutive samples divided by the number of days between the samples, was initially very high, and later stabilised at lower rates, which were similar in R1 and R2 (Fig. S6B).

3.5. Microbial community network

In the network analysis, nodes represent ASVs and edges represent positive correlations (co-occurrence) between pairs of ASVs. The network analysis showed that the microbiome could be divided into three dominant clusters and five minor clusters with only a few nodes, and the total number of edges (links between nodes) were 7136 (Fig. 5). Of the dominant clusters, cluster one, two and three had 191, 162 and 64 nodes, respectively. The minor clusters had 2–11 nodes. Cluster one decreased similarly in both reactors from the start-up and continued to decrease seemingly irrespective of the temperature decrease rate (Fig. 5). In contrast, cluster two increased in relative abundance until around day 82, whereafter the relative abundance remained high in R2 but decreased rapidly in R1. In cluster three, the relative abundance was very low at the beginning, and started to increase around day 82. Cluster

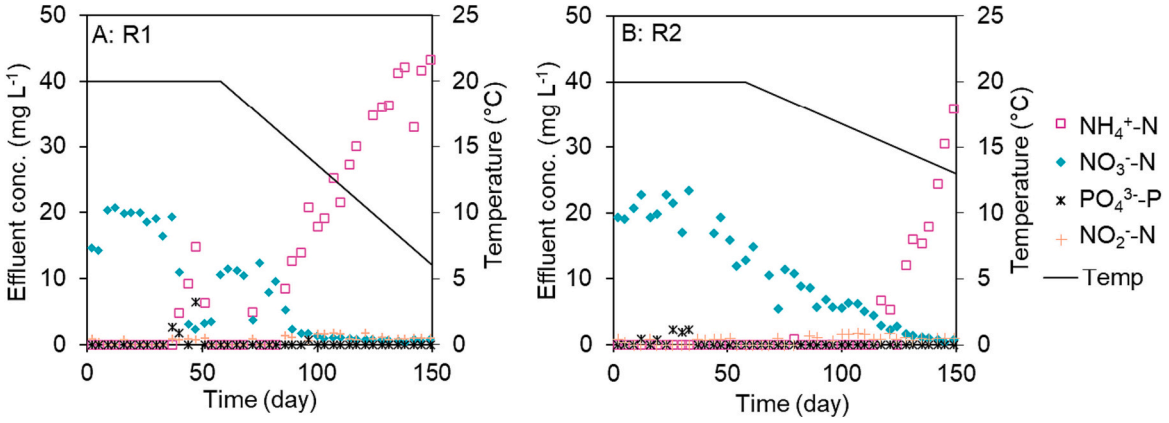

Fig. 2. Effluent concentrations of ammonium-, nitrate- and nitrite-nitrogen and phosphate-phosphorus and temperature in A) R1 and B) R2.

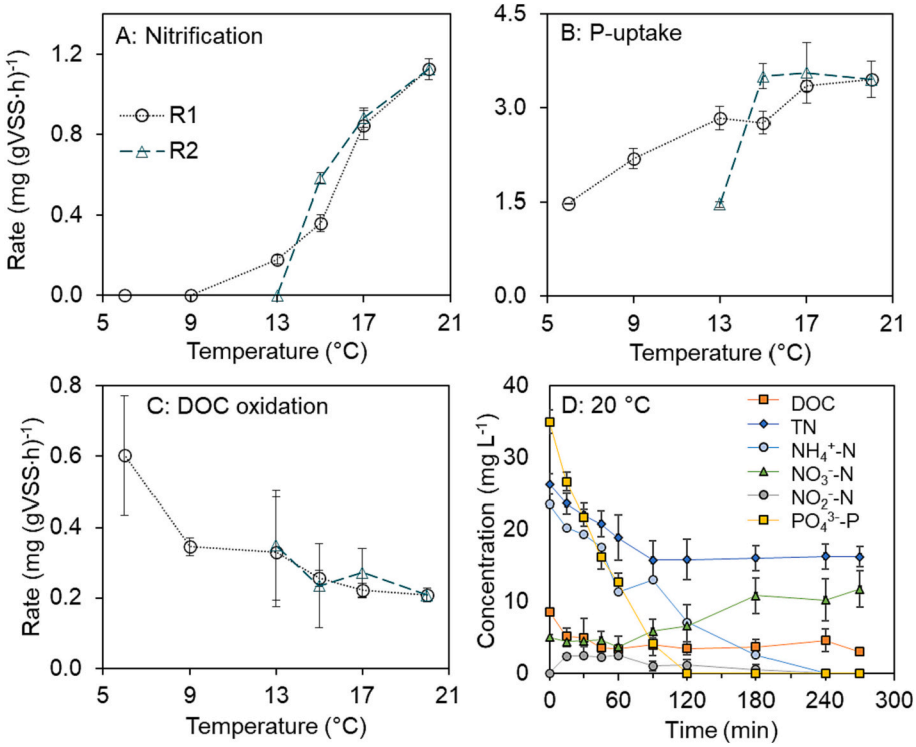

Fig. 3. A) Nitrification rate, B) phosphorus-uptake rate, and C) DOC oxidation rate in R1 and R2 as a function of temperature. Error bars indicate the standard deviation for each mean value (rate) from three cycle studies at each temperature. D) concentration profiles during the aeration phase at 20 °C, as averages from R1 and R2.

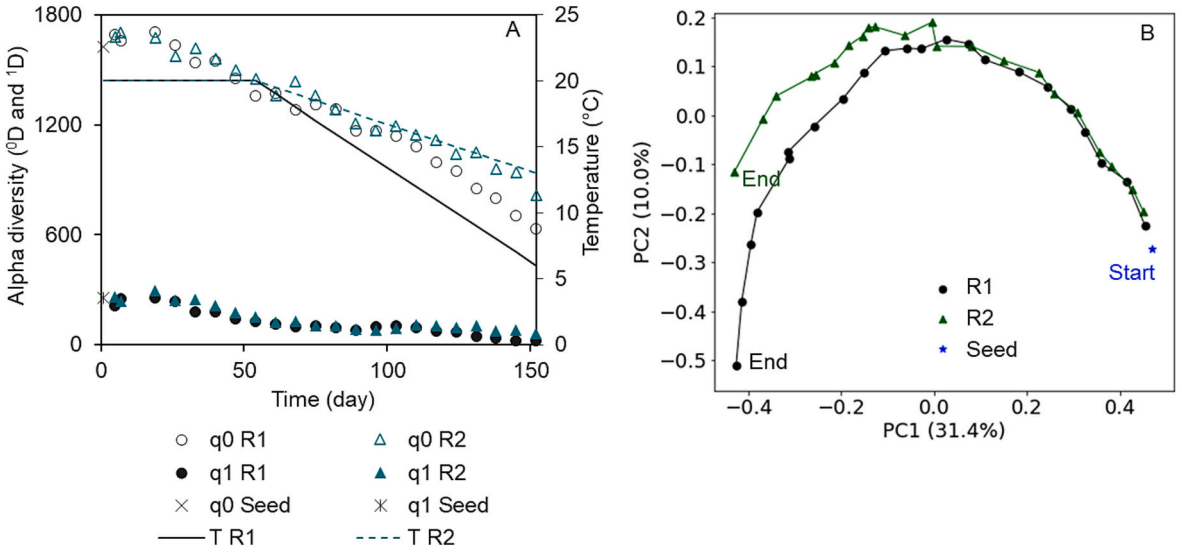

Fig. 4. A) Diversity (markers) and temperature (lines) in R1 and R2. B) PCoA plot (q = 1) of the microbial community composition in R1, R2 and the seed sample. Each point represents a sample. The lines connect samples collected at consecutive time points in the same reactor.

one was composed of, for example, *Terrimonas, Ferruginibacter* (aerobic heterotrophs), and *Tetrasphaera* (PAO), which all decreased in both reactors at similar rates. Cluster two was composed of, for example, Ca. Competibacter (GAO), *Nitrospira* (NOB) and *Flavobacterium* (aerobic heterotroph), and those are genera that were increasing until approximately 14–16 °C and was negatively influenced by lower temperatures. In contrast, cluster three was positively influenced by the temperature decrease and was composed of, for example, *Chryseobacterium*, *Cloacibacterium* (aerobic heterotrophs), *Acidaminobacter* (anaerobic heterotroph), Ca. Accumulibacter (PAO) and *Nitrosomonas* (AOB). Cluster three had higher abundance in R1 than R2 at the lower temperatures which indicated that the relative abundances of its members were increasing due to the lower temperatures.

The proximity of cluster two and three in the network plot suggests that some members in the clusters were positively correlated. The genera *Terrimonas* (cluster one, which decreased with time) and Ca. Competibacter (cluster two, which were temperature sensitive) had the highest degree of centrality. The degree centrality is related to the number of correlations an ASV has with other ASVs, and the index has been used to identify keystone species in ecological networks (Dunne

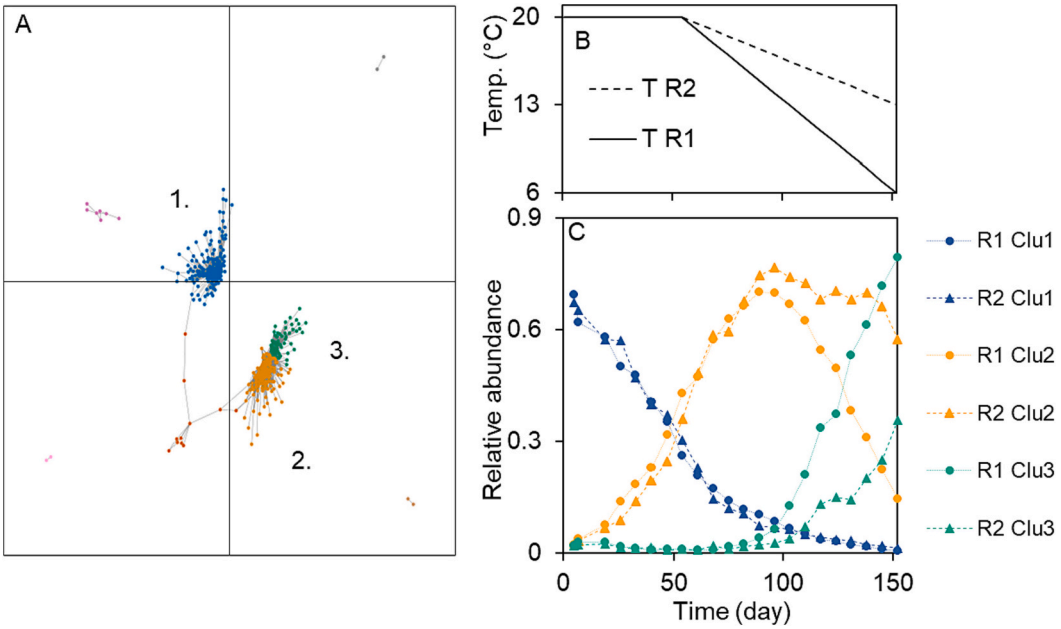

Fig. 5. A) Network positive correlations in both reactors' microbiome, B) the temperature alteration over time, and C) relative abundance of the sum of the ASVs in cluster one (blue), two (yellow) and thee (green). (For interpretation of the references to colour in this figure legend, the reader is referred to the web version of this article.)

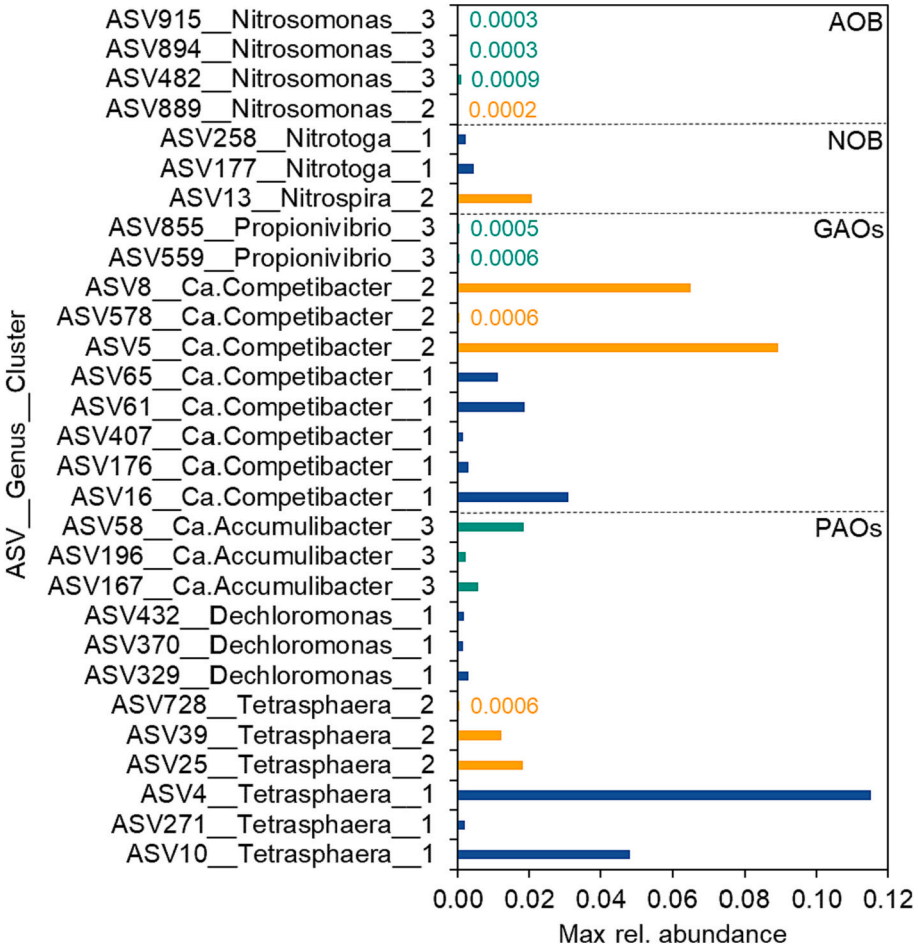

Fig. 6. Maximum relative abundance of each ASVs within the functional groups (PAOs, GAOs, AOB and NOB) in cluster one (blue), two (yellow) and three (green), in the network of positive correlations in both reactors' microbiomes. (For interpretation of the references to colour in this figure legend, the reader is referred to the web version of this article.)

et al., 2002). The five ASVs with the highest degree centrality in each cluster are presented in Table S6.

3.6. Impacts of altering temperature on abundance and dynamics of functional groups

3.6.1. Groups and genera

The relative abundances of the 20 most abundant ASVs in R1 and R2 are shown in Fig. S7. The seed and reactor microbial communities harboured the functional groups of PAOs, GAOs, AOB, and NOB. These groups showed dynamic relative abundances over time (Fig. S8), and all groups were found in at least two of the clusters in the microbial network (Fig. 6). Within the functional groups, different ASVs had different dynamics (Fig. S9), and were for some genera grouped to different network clusters (Fig. 6). The relative abundances of the functional groups during the temperature decrease period were analysed using Pearson's correlation test and paired sample *t*-test. When samples taken at the same temperature were compared, there were no significant differences between the relative abundances of functional groups in R1 and R2 ($p > 0.05$), except for PAOs ($p < 0.05$) which had higher abundances in R1 compared to R2 at the same temperature. The specific P-uptake rates in R1 were linearly correlated to the abundance of PAOs ($p < 0.05$), but not for R2.

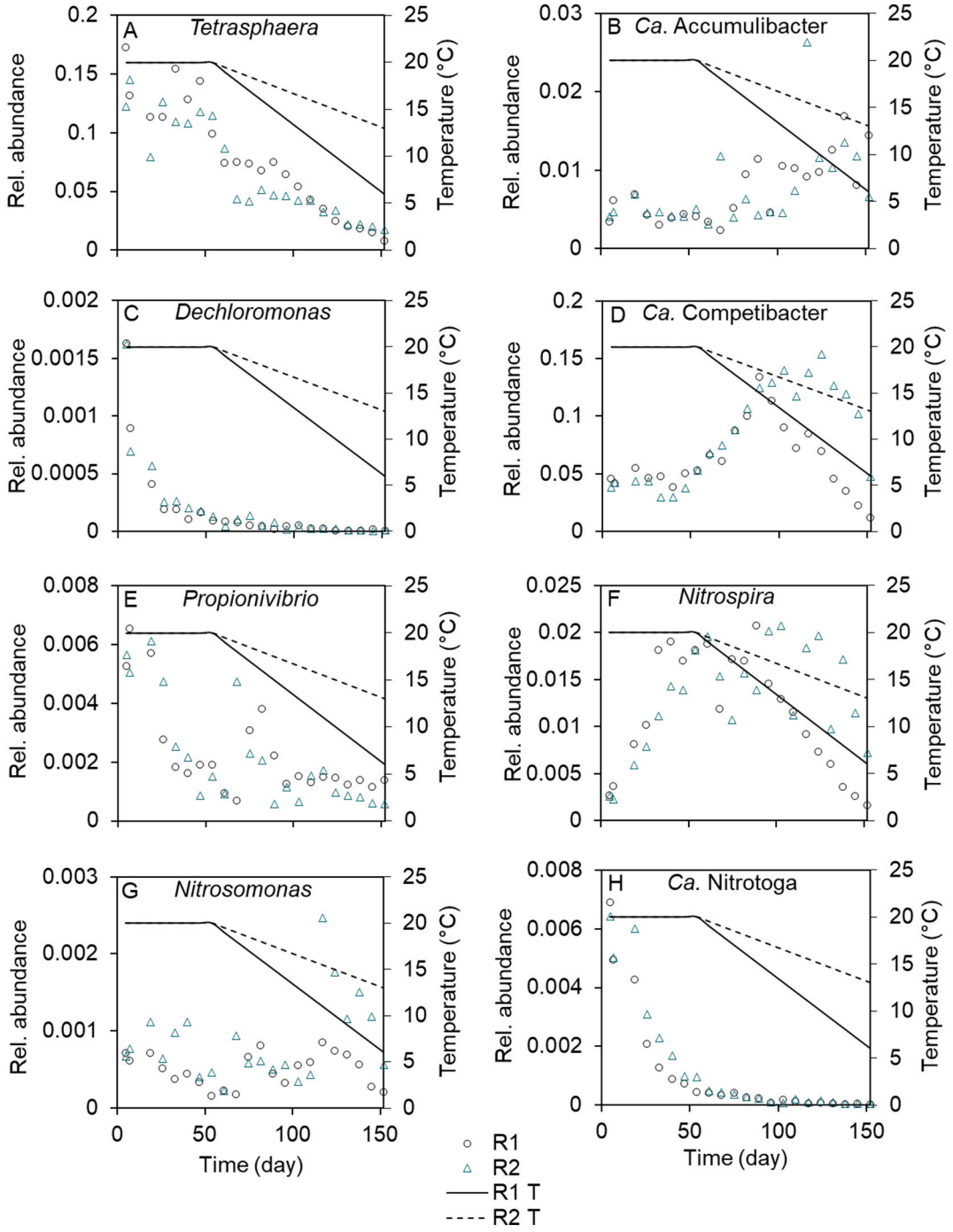

Fig. 7. Relative abundance in R1 (triangles) and R2 (circles) of A) *Tetrasphaera*, B) Ca. Accumulibacter, C) *Dechloromonas*, D) Ca. Competibacter, E) *Propionivibrio*, F) *Nitrospira,* G) *Nitrosomonas,* and H) Ca. Nitrotoga.

3.6.2. PAOs and GAOs

The PAOs as a group showed generally similar dynamics in R1 and R2 (Fig. S8), and genera within PAOs showed a variety of temporal dynamics. The PAOs were grouped into all three major clusters. For instance, the relative abundance of *Tetrasphaera* and *Dechloromonas* were decreasing with time (Fig. 7, and S10) and mainly found in cluster one, whereas Ca. Accumulibacter was increasing, grouped into cluster three (Fig. 6). A t-test for paired samples of the relative abundance of Ca. Accumulibacter showed no significant difference between R1 and R2 (Table S7), which means that the temperature decrease rate probably had little influence. *Tetrasphaera* was also found in cluster two, as some ASVs were peaking in relative abundance at temperatures around 14–16 °C (Fig. S9). During the temperature decrease period, the relative abundance of *Tetrasphaera* was not significantly different between R1 and R2 for samples taken the same day ($p > 0.05$, Table S6) despite the different temperatures.

The relative abundances of the GAOs were different in R1 and R2 on the same day ($p < 0.05$), but not at the same temperature, suggesting an influence of the temperature but no influence of the temperature decrease rate (Fig. S8). The GAOs had a similar dynamic in both reactors until day 89, when the decrease was more pronounced in R1. The DOC uptake during feeding was correlated to the relative abundance of GAOs in R1 ($p < 0.05$), but not for R2. Within the GAOs, the relative abundances of Ca. Competibacter were stable during the adaption period, increasing to a peak abundance around 15–16 °C, and decreasing at lower temperatures in both reactors (Fig. S10, S12). Ca. Competibacter was observed in both clusters one and two, and *Propionivibrio* was found in cluster three (Fig. 6). The relative abundance of the main *Propionivibrio* (ASV96) increased with an unpredictable manner with respect to temperature and time, and hence did not affiliate with any of the clusters (Fig. S9). However, a couple of minor ASVs within *Propionivibrio* belonged to cluster three, increasing at lower temperatures.

3.6.3. Nitrifiers

The relative abundance of AOB, the genus *Nitrosomonas*, was low in both reactors and showed a similar dynamic in the reactors until day 110, whereafter the relative abundance was higher in R2 ($p < 0.05$) which also had a higher temperature (Fig. 7, S8). ASVs within *Nitrosomonas* were mainly found in cluster three (Fig. 7). The abundance of NOB increased until the temperature experimental period started, when it decreased fast in R1 and was more fluctuating but decreasing also in R2. *Nitrospira* (NOB/Comammox) had higher relative abundance in R2 than R1 when comparing the same day, but not when comparing abundances at the same temperature (Fig. 7 and S9). The relative abundance of *Nitrospira*, which was only detected as one ASV, was also varying to a higher extent in R2, whereas in R1 the decrease was steady at temperatures below 15 °C. One ASV of *Nitrosomonas* and *Nitrospira* were grouped into cluster two, and followed the dynamics of the cluster with a peak in relative abundance around 14–16 °C. The relative abundance of Ca. Nitrotoga (NOB), found in cluster one (Fig. 6), was similar in both reactors ($p > 0.05$) and was decreasing fast already at 20 °C (Fig. 7), indicating that time was more important than temperature. The nitrification rates could not be fitted by linear regression with the relative abundance of AOB and/or NOB ($p > 0.05$).

3.6.4. Denitrifiers and aerobic heterotrophs

The detected canonical denitrifiers were *Thaurea*, *Zoogloea*, Ca. Accumulibacter, Ca. Competibacter, *Flavobacterium*, *Rhodoferax*, *Dechloromonas*, *Sulfuritalea*, *Thermomonas* and *Haliangium*, but also other bacteria may carry the genes for full or partial denitrification (Harter et al., 2016; McIlroy et al., 2016). The denitrifiers were grouped into all the three clusters. *Thauera* was decreasing to relative abundances close to zero even before the temperatures were decreased (not grouped to the major clusters), whereas the relative abundances of *Zoogloea* were first decreasing, but later increasing at lower temperatures (cluster three). The aerobic heterotroph *Flavobacterium,* with ASVs found in both clusters two and three, had a peak of relative abundance around 13–14 °C (Fig. S10). Another aerobic heterotroph, *Chryseobacterium*, increased from very low abundances to remarkably 40 % in R1 when the temperature had reached 6 °C (Fig. S10). Several other aerobic heterotrophs such as *Methylotenera* and *Cloacibacterium*, as well as the fermentative *Acidaminobacter* (anaerobic fermentation utilizing proteins/amino acids as substrate (Dueholm et al., 2022), were also increasing with decreasing temperature and were grouped to cluster three. The aerobic heterotrophs *Terrimonas* and *Ferruginibacter*, found in cluster one, decreased over time (Fig. S11).

4. Discussion

4.1. Influence of temperature on microbial community structure

The alpha diversity at $q = 0$ and $q = 1$ were decreasing at a similar rate in both reactors until around day 110 (Fig. 4A) when the diversity was lower in R1 (13 °C) than R2 (16 °C). This indicates that at temperatures below 13 °C, ASVs were more severely washed out. Previously, a constant low temperature of 7 °C also caused lower species richness in AGS, compared to a constant temperature of 26 °C (Muñoz-Palazon et al., 2022). Reduced diversity and evenness indicate that certain abundant ASVs were preferred at lower temperatures, while others decayed or were eliminated with decreasing temperatures.

Furthermore, R2 had lower species richness and alpha diversity than R1 when comparing the samples collected at the same temperature (Fig. S5), suggesting that operation time alone was driving a decrease in diversity. A decreasing diversity with time at lab conditions could be expected due to the lack of immigration of new species from the influent wastewater. Also, the microbial communities were exposed to less fluctuations and disturbances in the lab-scale reactors, compared with the full-scale plant from where the inoculum was taken, leading to fewer niches (Shea and Chesson, 2002).

In the PCoA (Fig. 4B), R1 separated from R2 around day 68, indicating that the difference in temperature decrease rates was driving this shift in community structure. Interestingly, the community composition in both reactors changed at a similar rate despite the differences in temperature, which indicates that other factors than temperature decrease rate had more influence on the rate of community change.

The network analysis revealed three dominant clusters with positive correlations, which showed a temperature related succession dynamics in microbial community composition between clusters two and three (Fig. 5). The similarity between R1 and R2 for cluster one suggests that the relative abundance of those ASVs decreased due to other factors than the temperature. This means that the microbial communities were subject to two major processes: a temperature induced shift and a loss of microorganisms due to less competitiveness at the environmental conditions present in the laboratory. The environmental conditions were for example 20 °C during the adaption period, synthetic wastewater (Table 1), controlled pH, and few fluctuations. Cluster one, in which for example *Terrimonas, Ferruginibacter*, and *Tetrasphaera* were grouped, was decreasing irrespective of the temperature (Fig. 5). *Terrimonas* was previously found in full-scale AGS reactors and related to hydrolysation of complex substrates which was scarce in the lab-feed (Ekholm et al., 2022; Toja Ortega et al., 2021b). *Ferruginibacter* also hydrolyse organic compounds (Lim et al., 2009). *Tetrasphaera* is commonly found in full-scale reactors (Liu et al., 2022a; Stokholm-Bjerregaard et al., 2017), where the influent wastewater is more complex than synthetic wastewater often applied in lab-scale studies (Adler and Holliger, 2020). Hence, these dynamics might depend on the loss of advantage of these members to ferment macromolecules and were outcompeted by others who had an advantage at VFA-rich conditions. Previous research found that the complexity of the synthetic wastewater influenced the microbial community composition (Adler and Holliger, 2020) and a lower complexity decreased the diversity (Layer et al., 2019). The decreased diversity of the microbial community might influence the ecosystem

functions negatively, eventually leading to a more specialised community. This observation is important as it highlights differences in community composition and competitional dynamics caused by laboratory conditions.

Both PAOs and GAOs were found in all clusters, and the AOB and NOB were both found in two clusters (AOB 2 and 3, and NOB 1 and 2) in the network analysis (Fig. 6), indicating a variety of responses within the groups to the decreasing temperatures, and other reactor conditions.

4.2. Influence of temperature on nutrient removal

4.2.1. Phosphorus removal

Different ASVs within *Tetrasphaera* responded differently to the temperature decrease as they were grouped into both cluster one and two (Fig. 6). The most abundant ASV was grouped to cluster one, which largely influenced the dynamics of *Tetrasphaera*; a vast decrease which was similar in the two reactors. In both reactors, the P-uptake rate decreased with the temperature, and the anaerobic uptake of organic matter also decreased during the study. Despite the overall decrease of the relative abundance of PAOs, the decreasing temperatures did not impact the ability of the reactors to remove phosphate completely. In contrast, the genus Ca. Accumulibacter, known to grow on short-chain fatty acids and commonly found in lab-scale reactors (Layer et al., 2019), was increasing with time in the reactors (Fig. 7), and grouped to cluster three (Fig. 6). As the increase was more pronounced in R1 (Fig. S10) and Ca. Accumulibacter was grouped to cluster three, this suggests that Ca. Accumulibacter was favoured by the lower temperatures (<13 °C). These results are supported by a recent study of activated sludge, where it was found that the relative abundance of Ca. Accumulibacter increased at 10 °C compared to 20 °C (Liu et al., 2022a). Furthermore, in a previous study of AGS, the relative abundance of Ca. Accumulibacter was decreasing from 35 % to <5 % when the wastewater composition changed from monomeric to complex carbon source, suggesting a strong influence of the carbon source (Adler and Holliger, 2020). The large decrease in abundance of *Tetrasphaera* (Fig. 7) might be the reason for the lower P-uptake rate in R2 at 13 °C, compared to R1 at the same temperature (Fig. 3B). The read counts of an ASV are however not necessary reflecting the real number of bacteria present in a sample. The 16S rRNA gene amplicon sequencing analysis has been widely used and has given valuable information, but it also has important limitations, due to the differences in affinity for primers to bind to specific bacteria leading to higher amplification of some sequences (Poretsky et al., 2014). This may lead to an underestimated relative abundance of Ca. Accumulibacter according to a recent study (Kleikamp et al., 2023). The dynamics between samples in relative abundance should, however, reflect the real dynamic, as the possible bias can be assumed to be similar in all samples.

Within the GAOs, Ca. Competibacter first increased to a peak abundance around 15–16 °C whereafter the abundance decreased (Fig. S10 and S12). This was likely due to a highly abundant ASV within Ca. Competibacter which was grouped to cluster two. These dynamics are in accordance with previous research where Ca. Competibacter was found to be insensitive to temperatures 15–35 °C, but showed lower activity (Lopez-Vazquez et al., 2009) and relative abundance (Yuan et al., 2019) at 10 °C. Several ASVs within Ca. Competibacter were also grouped to cluster one (Fig. 6), indicating that other factors than the temperature had a negative influence on the abundances. One factor could be the composition of the synthetic wastewater, which had a higher COD/P ratio compared to the influent at the WWTP where the inoculum was collected (Ekholm et al., 2022). A couple of ASVs within *Propionivibrio* (Albertsen et al., 2016) were grouped to cluster three, which increased the abundance at lower temperatures (Figs. 5 and 6). This supports a previous study where *Propionivibrio* was found abundant at low temperature (10 °C) in an activated sludge SBR (Li et al., 2019). The P-uptake rate at 20 °C (3.45 ± 0.29 mg PO_4^{3-}-P g VSS^{-1} h^{-1}) was in accordance with previous results (Bassin et al., 2012), which were 3.5–3.9 mg PO_4^{3-}-P g VSS^{-1} h^{-1}. In the aforementioned study, several operational parameters were similar to this study; the seeding sludge was from an AGS pilot-plant treating municipal wastewater, controlled SRT of 30 days, and similar DO and COD concentrations.

The denitrification improved during the adaption period and down to approximately 15 °C in both reactors (Figs. 2 and S2), which possibly could be explained by the similar dynamics in the abundance of Ca. Competibacter (Fig. 7), recently shown to have a large denitrifying capacity (Dan et al., 2021). Interestingly, the strictly anaerobic fermentative *Acidaminobacter* was increasing along the decreasing temperature and had a high degree centrality in cluster three in the network analysis. This suggests that *Acidaminobacter* was successfully competing with PAOs and GAOs for organic carbon in the anaerobic feeding phase, as several abundant ASVs of PAOs and GAOs were found in the other clusters.

The concentration of MLSS in both reactors increased along the experiment. Since phosphorus is bound in the bacterial cells, higher MLSS concentration would lead to increased amount of phosphorus removed with the discharged solids. However, the cycle studies showed stable release of phosphate also below 15 °C and in R1 it was only slightly reduced at 9 and 6 °C (Fig. S3). This together with the abundance of PAOs in the biomass confirm that the activity of the phosphorus accumulating microorganisms is responsible for the phosphorus removal also at low temperatures.

4.2.2. Nitrogen removal

The nitrification rate at 20 °C was 1.1 ± 0.05 mg NH_4^+-N g VSS^{-1} h^{-1} which is close to the result by Bassin et al. (2012), an AGS lab-scale study at 20 °C where rates of 0.9–1.1 mg NH_4^+-N g VSS^{-1} h^{-1} were obtained. The similarity suggests reproducibility of the nitrification rates. Lowering of the temperature led to significantly decreased nitrification rates, but this trend was not directly reflected in the abundance of AOB and NOB (Fig. 7). However, failure of nitrification during low temperatures despite constant abundances was previously observed in activated sludge (Johnston et al., 2019), possibly explained by variations in specific activity or even undiscovered or unidentified AOB (Ali et al., 2019). ASVs within the AOB *Nitrosomonas* were grouped to both cluster two and three (Fig. 6), showing that different ASVs had various responses to the decreasing temperatures. The relative abundance of *Nitrosomonas* was generally higher in R2 than R1 in samples taken at the same temperature, suggesting that the slower temperature decrease rate was in favour for *Nitrosomonas*. Indeed, the nitrification rate was higher in R2 than R1 at 15 °C, and at this temperature the relative abundance of *Nitrosomonas* was remarkably higher in R2 (0.0016) compared to R1 (0.00044). On the contrary, at 13 °C the nitrification rate was higher in R1 (zero in R2) (Fig. 3), but the reactors had a similar relative abundance of *Nitrosomonas*. The difference in the nitrification rates at 13 °C could possibly be explained by *Nitrospira* performing complete ammonium oxidation. Nitrifiers and aerobic heterotrophs both utilise oxygen, and as nitrifiers have a lower affinity for the oxygen they are poor competitors. As the temperature decreased, more organic matter was converted in the aerobic phase, which likely increased the competition for the more slowly growing nitrifiers (Gieseke et al., 2001) and the nitrification conversion rates decreased. The NOB Ca. Nitrotoga was found in cluster one (Fig. 6) and was abundant in the seeding granules but decreased fast in both reactors already during the adaption period. At the same time, *Nitrospira*, grouped to cluster two, was increasing (Fig. 7). This suggests that during the adaption at 20 °C, *Nitrospira* was favoured over Ca. Nitrotoga, as the latter has been identified as a cold-adapted NOB (Lücker et al., 2015; Spieck et al., 2021) and might therefore have higher competitiveness at lower temperatures.

From a practical point of view, an increase of SRT and/or the biomass concentration could perhaps mitigate the loss of nitrification, by increasing the numbers of AOB and NOB. In AGS systems, there is a distribution of SRTs within the same reactor since larger and heavier granules can remain in the lower part of the reactor for a longer time (Ali

et al., 2019). By applying selective biomass removal from the top of the reactor, granules with longer SRT are maintained (Winkler et al., 2011). Another countermeasure to promote the nitrification would be to increase the DO concentration, as suggested for integrated fixed film activated sludge systems (Regmi et al., 2011), although the oxygen transfer rate increases at lower temperatures due to the higher DO saturation concentration (Strubbe et al., 2023).

4.3. Influence of temperature on granule characteristics

The different carbon sources diffused to different degrees or were hydrolyzed at the granule surface, which was reflected in filamentous outgrowths at the granule surface and also the growth of floccular sludge (Fig. S1). Filamentous outgrowth was previously associated with worsening of settling properties and disintegration of granules (de Kreuk et al., 2010; Moura et al., 2018) and filamentous bacteria are commonly known to cause bulking sludge in activated sludge systems (Martins et al., 2004). The relative abundance of *Chryseobacterium*, which harbours several filamentous clades, increased very fast up to 40 % in R1 and to 12 % in R2 (Fig. S10), corresponding in time to increasing conversion of organic matter in the aerobic phase. *Leucobacter*, *Limnohabitants* and *Cloacibacterium* were also increasing at lower temperatures, probably related to competitive advantages due to faster growth of these aerobic heterotrophs. *Chryseobacterium* and *Leucobacter* seem to benefit at cold temperatures, as they were previously found in high relative abundances in a lab-scale AGS reactor operated at 7 °C (Gonzalez-Martinez et al., 2017). Despite the increase of aerobic heterotrophs, the granule stability was kept and the SVI stayed low (Fig. 1), presumably depending on the relatively high abundance of PAOs and GAOs, which are found to be essential for granulation (Adler and Holliger, 2020; de Kreuk and van Loosdrecht, 2004).

The average granule diameter increased along the experiment, in spite of the lowering of temperature. What factors influence the granule size is not fully understood, and is a complex result of the environmental conditions in the reactor that influence the development of granule composition and structure (e.g. availability of substrate for microbial growth and shear forces). For example, as the water temperature decreases, the hydrodynamic shear force increases and at 6 °C, it is approximately 20 % higher than at 20 °C. In R1, the granules remained compact but dropped in size when the temperature reached 9 °C, possibly as the result of applied increased shear forces (Table 1, Fig. S1).

5. Conclusions

The influences of decreasing temperatures in two lab-scale reactors were investigated, which revealed pronounced dynamics in the microbial communities and the nutrient removal performances. The microbial community could be clustered into three major clusters in a network of positive correlations, expressing two major drivers for shift in the microbiome: a temperature dependent replacing dynamic of two clusters, and “washing out” of bacteria in the third cluster, likely caused by the composition of the synthetic wastewater. The lower temperatures in R1 led to lower species richness, higher dissimilarity (compared with the seed) and lower evenness compared to R2. The temperature decrease rate was found to have limited influence on the reactor performance and microbial community, rather the temperature itself showed a large influence. Members within the functional groups of PAOs, GAOs, AOB, NOB, and denitrifiers were differently influenced by the temperature. Most process performance sensitive were the AOB and NOB, resulting in decreasing nitrification rates. Differences in the biomass specific removal rates of ammonium and phosphate could possibly be explained by the different relative abundance of ASVs belonging to the functional groups. The removal of organic matter and phosphorus was high and stable, and the settling remained fast despite the temperature alteration and large community dynamics.

CRediT authorship contribution statement

Jennifer Ekholm: Writing – review & editing, Writing – original draft, Methodology, Investigation, Formal analysis, Conceptualization. **Cecilia Burzio:** Methodology, Investigation, Formal analysis. **Amir Saeid Mohammadi:** Resources. **Oskar Modin:** Writing – review & editing, Data curation. **Frank Persson:** Writing – review & editing, Supervision, Methodology, Funding acquisition, Conceptualization. **David J.I. Gustavsson:** Writing – review & editing, Supervision, Project administration, Methodology, Funding acquisition, Conceptualization. **Mark de Blois:** Writing – review & editing, Supervision, Methodology, Funding acquisition, Conceptualization. **Britt-Marie Wilén:** Writing – review & editing, Supervision, Methodology, Investigation, Funding acquisition, Conceptualization.

Declaration of competing interest

The authors declare that they have no known competing financial interests or personal relationships that could have appeared to influence the work reported in this paper.

Data availability

Data will be made available on request.

Acknowledgments

This study was funded by J. Gust. Richert foundation (2021-00724), the Swedish Water & Wastewater Association (SVU), Sweden Water Research and the Swedish municipal WWTP operators Uppsala Vatten och Avfall, and Gryaab and Käppala Association. Members of the project are as well Chalmers University of Technology, H2OLAND, the municipality of Strömstad, the municipality of Tanum, TU Delft and Royal HaskoningDHV and the municipality of Västervik.

Appendix A. Supplementary data

Supplementary data to this article can be found online at https://doi.org/10.1016/j.biteb.2024.101792.

References

Adams, H.E., Crump, B.C., Kling, G.W., 2010. Temperature controls on aquatic bacterial production and community dynamics in arctic lakes and streams. Environ. Microbiol. 12 (5), 1319–1333. https://doi.org/10.1111/j.1462-2920.2010.02176.x.

Adler, A., Holliger, C., 2020. Multistability and reversibility of aerobic granular sludge microbial communities upon changes from simple to complex synthetic wastewater and back. Front. Microbiol. 11, 574361 https://doi.org/10.3389/fmicb.2020.574361.

Alawi, M., Lipski, A., Sanders, T., Eva Maria, P., Spieck, E., 2007. Cultivation of a novel cold-adapted nitrite oxidizing betaproteobacterium from the Siberian Arctic. ISME J. 1 (3), 256–264. https://doi.org/10.1038/ismej.2007.34.

Albertsen, M., McIlroy, S.J., Stokholm-Bjerregaard, M., Karst, S.M., Nielsen, P.H., 2016. “Candidatus Propionivibrio aalborgensis”: a novel glycogen accumulating organism abundant in full-scale enhanced biological phosphorus removal plants. Front. Microbiol. 7, 1033. https://doi.org/10.3389/fmicb.2016.01033.

Ali, M., Wang, Z., Salam, K.W., Hari, A.R., Pronk, M., van Loosdrecht, M.C.M., Saikaly, P. E., 2019. Importance of species sorting and immigration on the bacterial assembly of different-sized aggregates in a full-scale aerobic granular sludge plant. Environ. Sci. Technol. 53 (14), 8291–8301. https://doi.org/10.1021/acs.est.8b07303.

APHA, 2005. Standard Methods for the Examination of Water and Wastewater. American Public Health Association, Washington DC.

Arnell, M., Ahlström, M., Wärff, C., Saagi, R., Jeppsson, U., 2021. Plant-wide modelling and analysis of WWTP temperature dynamics for sustainable heat recovery from wastewater. Water Sci. Technol. 84 (4), 1023–1036. https://doi.org/10.2166/wst.2021.277.

Arrojo, B., Figueroa, M., Mosquera-Corral, A., Campos, J.L., Méndez, R., 2008. Influence of gas flow-induced stress on the operation of the Anammox process in a SBR. Chemosphere 72 (11), 1687–1693. https://doi.org/10.1016/j.chemosphere.2008.05.017.

Bassin, J.P., Kleerebezem, R., Dezotti, M., van Loosdrecht, M.C.M., 2012. Simultaneous nitrogen and phosphate removal in aerobic granular sludge reactors operated at

different temperatures. Water Res. 46 (12), 3805–3816. https://doi.org/10.1016/j.watres.2012.04.015.
Callahan, B.J., McMurdie, P.J., Rosen, M.J., Han, A.W., Johnson, A.J.A., Holmes, S.P., 2016. DADA2: High-resolution sample inference from Illumina amplicon data. Nat. Methods 13 (7), 581–583. https://doi.org/10.1038/nmeth.3869.
Chao, A., Chiu, C.-H., Jost, L., 2014. Unifying species diversity, phylogenetic diversity, functional diversity, and related similarity and differentiation measures through hill numbers. Annu. Rev. Ecol. Evol. Syst. 45 (1), 297–324. https://doi.org/10.1146/annurev-ecolsys-120213-091540.
la Cour Jansen, J., Kristensen, G.H., Laursen, K.D., 1992. Activated sludge nitrification in temperate climate. Water Sci. Technol. 25 (4–5), 177–184.
Dan, Q., Peng, Y., Wang, B., Wang, Q., Sun, T., 2021. Side-stream phosphorus famine selectively strengthens glycogen accumulating organisms (GAOs) for advanced nutrient removal in an anaerobic-aerobic-anoxic system. Chem. Eng.J. 420, 129554 https://doi.org/10.1016/j.cej.2021.129554.
Dueholm, M.K.D., Nierychlo, M., Andersen, K.S., Rudkjøbing, V., Knutsson, S., Arriaga, S., Bakke, R., Boon, N., Bux, F., Christensson, M., Chua, A.S.M., Curtis, T.P., Cytryn, E., Erijman, L., Etchebehere, C., Fatta-Kassinos, D., Frigon, D., Garcia-Chaves, M.C., Gu, A.Z., Horn, H., Jenkins, D., Kreuzinger, N., Kumari, S., Lanham, A., Law, Y., Leiknes, T., Morgenroth, E., Muszyński, A., Petrovski, S., Pijuan, M., Pillai, S.B., Reis, M.A.M., Rong, Q., Rossetti, S., Seviour, R., Tooker, N., Vainio, P., van Loosdrecht, M., Vikraman, R., Wanner, J., Weissbrodt, D., Wen, X., Zhang, T., Nielsen, P.H., Albertsen, M., Nielsen, P.H., Mi, D.A.S.G.C., 2022. MiDAS 4: a global catalogue of full-length 16S rRNA gene sequences and taxonomy for studies of bacterial communities in wastewater treatment plants. Nat. Commun. 13 (1), 1908. https://doi.org/10.1038/s41467-022-29438-7.
Dunne, J.A., Williams, R.J., Martinez, N.D., 2002. Network structure and biodiversity loss in food webs: robustness increases with connectance. Ecol. Lett. 5 (4), 558–567. https://doi.org/10.1046/j.1461-0248.2002.00354.x.
Ekholm, J., Persson, F., de Blois, M., Modin, O., Pronk, M., van Loosdrecht, M., Suarez, C., Gustavsson, D.J., Wilén, B.-M., 2022. Full-scale aerobic granular sludge for municipal wastewater treatment–granule formation, microbial succession, and process performance. Environ. Sci.: Water Res. Technol. 8 (12), 3138–3154. https://doi.org/10.1039/d2ew00653g.
Friedman, J., Alm, E.J., 2012. Inferring correlation networks from genomic survey data. PLoS Comput. Biol. 8 (9), 1002687. https://doi.org/10.1371/journal.pcbi.1002687.
Gao, H., Mao, Y., Zhao, X., Liu, W.T., Zhang, T., Wells, G., 2019. Genome-centric metagenomics resolves microbial diversity and prevalent truncated denitrification pathways in a denitrifying PAO-enriched bioprocess. Water Res. 155, 275–287. https://doi.org/10.1016/j.watres.2019.02.020.
Gieseke, A., Purkhold, U., Wagner, M., Amann, R., Schramm, A., 2001. Community structure and activity dynamics of nitrifying bacteria in a phosphate-removing biofilm. Appl. Environ. Microbiol. 67 (3), 1351–1362. https://doi.org/10.1128/AEM.67.3.1351-1362.200.
Gonzalez-Martinez, A., Muñoz-Palazon, B., Rodriguez-Sanchez, A., Maza-Márquez, P., Mikola, A., Gonzalez-Lopez, J., Vahala, R., 2017. Start-up and operation of an aerobic granular sludge system under low working temperature inoculated with cold-adapted activated sludge from Finland. Bioresour. Technol. 239, 180–189. https://doi.org/10.1016/j.biortech.2017.05.037.
Gonzalez-Martinez, A., Muñoz-Palazon, B., Maza-Márquez, P., Rodriguez-Sanchez, A., Gonzalez-Lopez, J., Vahala, R., 2018. Performance and microbial community structure of a polar Arctic Circle aerobic granular sludge system operating at low temperature. Bioresour. Technol. 256, 22–29. https://doi.org/10.1016/j.biortech.2018.01.147.
Hagberg, A., Swart, P., Chult, S.D., 2008. Exploring Network Structure, Dynamics, and Function Using NetworkX, Los Alamos National Lab.(LANL), Los Alamos, NM (United States).
Hamza, R., Rabii, A., Ezzahraoui, F.-z., Morgan, G. and Iorhemen, O.T., 2022. A review of the state of development of aerobic granular sludge technology over the last 20 years: Full-scale applications and resource recovery. Case Studies Chem. Environ. Eng. 5, 100173. doi:https://doi.org/10.1016/j.cscee.2021.100173.
Han, F., Zhang, M., Liu, Z., Han, Y., Li, Q., Zhou, W., 2022. Enhancing robustness of halophilic aerobic granule sludge by granular activated carbon at decreasing temperature. Chemosphere 292, 133507. https://doi.org/10.1016/j.chemosphere.2021.133507.
Harter, J., Weigold, P., El-Hadidi, M., Huson, D.H., Kappler, A., Behrens, S., 2016. Soil biochar amendment shapes the composition of N_2O-reducing microbial communities. Sci. Total Environ. 562, 379–390. https://doi.org/10.1016/j.scitotenv.2016.03.220.
Johnston, J., LaPara, T., Behrens, S., 2019. Composition and dynamics of the activated sludge microbiome during seasonal nitrification failure. Sci. Rep. 9 (1), 4565. https://doi.org/10.1038/s41598-019-40872-4.
Jost, L., 2006. Entropy and diversity. Oikos 113 (2), 363–375. https://doi.org/10.1111/j.2006.0030-1299.14714.x.
Kleikamp, H.B.C., Grouzdev, D., Schaasberg, P., van Valderen, R., van der Zwaan, R., van de Wijgaart, R., Lin, Y., Abbas, B., Pronk, M., van Loosdrecht, M.C.M., Pabst, M., 2023. Metaproteomics, metagenomics and 16S rRNA sequencing provide different perspectives on the aerobic granular sludge microbiome. Water Res. 246, 120700 https://doi.org/10.1016/j.watres.2023.120700.
de Kreuk, M.K., van Loosdrecht, M.C.M., 2004. Selection of slow growing organisms as a means for improving aerobic granular sludge stability. Water Sci. Technol. 49 (11−12), 9–17. https://doi.org/10.2166/wst.2004.0792.
de Kreuk, M.K., Kishida, N., Tsuneda, S., van Loosdrecht, M.C.M., 2010. Behavior of polymeric substrates in an aerobic granular sludge system. Water Res. 44 (20), 5929–5938. https://doi.org/10.1016/j.watres.2010.07.033.
Kruglova, A., Kesulahti, J., Minh Le, K., Gonzalez-Martinez, A., Mikola, A., Vahala, R., 2020. Low-temperature adapted nitrifying microbial communities of Finnish wastewater treatment systems. Water 12 (9), 2450. https://doi.org/10.3390/w12092450.
Layer, M., Adler, A., Reynaert, E., Hernandez, A., Pagni, M., Morgenroth, E., Holliger, C., Derlon, N., 2019. Organic substrate diffusibility governs microbial community composition, nutrient removal performance and kinetics of granulation of aerobic granular sludge. Water Res X 4, 100033. https://doi.org/10.1016/j.wroa.2019.100033.
Leventhal, G.E., Boix, C., Kuechler, U., Enke, T.N., Sliwerska, E., Holliger, C., Cordero, O. X., 2018. Strain-level diversity drives alternative community types in millimetre-scale granular biofilms. Nat. Microbiol. 3 (11), 1295–1303. https://doi.org/10.1038/s41564-018-0242-3.
Li, C., Liu, S., Ma, T., Zheng, M., Ni, J., 2019. Simultaneous nitrification, denitrification and phosphorus removal in a sequencing batch reactor (SBR) under low temperature. Chemosphere 229, 132–141. https://doi.org/10.1016/j.chemosphere.2019.04.185.
Lim, J.H., Baek, S.-H., Lee, S.-T., 2009. Ferruginibacter alkalilentus gen. nov., sp. nov. and Ferruginibacter lapsinanis sp. nov., novel members of the family 'Chitinophagaceae' in the phylum Bacteroidetes, isolated from freshwater sediment. Int. J. Syst. Evol. Microbiol. 59 (10), 2394–2399. https://doi.org/10.1099/ijs.0.009480-0.
Liu, H., Zeng, W., Meng, Q., Fan, Z., Peng, Y., 2022a. Phosphorus removal performance, intracellular metabolites and clade-level community structure of Tetrasphaera-dominated polyphosphate accumulating organisms at different temperatures. Sci. Total Environ. 842, 156913 https://doi.org/10.1016/j.scitotenv.2022.156913.
Liu, Q., Peng, Y., Zhao, Y., Zhao, Q., Li, X., Zhang, Q., Sui, J., Wang, C., Li, J., 2022b. Excellent anammox performance driven by stable partial denitrification when encountering seasonal decreasing temperature. Bioresour. Technol. 364, 128041 https://doi.org/10.1016/j.biortech.2022.128041.
Lopez-Vazquez, C.M., Hooijmans, C.M., Brdjanovic, D., Gijzen, H.J., van Loosdrecht, M. C.M., 2009. Temperature effects on glycogen accumulating organisms. Water Res. 43 (11), 2852–2864. https://doi.org/10.1016/j.watres.2009.03.038.
Lücker, S., Schwarz, J., Gruber-Dorninger, C., Spieck, E., Wagner, M., Daims, H., 2015. Nitrotoga-like bacteria are previously unrecognized key nitrite oxidizers in full-scale wastewater treatment plants. ISME J. 9 (3), 708–720. https://doi.org/10.1038/ismej.2014.158.
Martins, A.M.P., Pagilla, K., Heijnen, J.J., van Loosdrecht, M.C.M., 2004. Filamentous bulking sludge—a critical review. Water Res. 38 (4), 793–817. https://doi.org/10.1016/j.watres.2003.11.005.
McIlroy, S.J., Starnawska, A., Starnawski, P., Saunders, A.M., Nierychlo, M., Nielsen, P. H., Nielsen, J.L., 2016. Identification of active denitrifiers in full-scale nutrient removal wastewater treatment systems. Environ. Microbiol. 18 (1), 50–64. https://doi.org/10.1111/1462-2920.12614.
Modin, O., Liébana, R., Saheb-Alam, S., Wilén, B.-M., Suarez, C., Hermansson, M., Persson, F., 2020. Hill-based dissimilarity indices and null models for analysis of microbial community assembly. Microbiome 8 (1), 132. https://doi.org/10.1186/s40168-020-00909-7.
Moura, L.L., Duarte, K.L.S., Santiago, E.P., Mahler, C.F., Bassin, J.P., 2018. Strategies to re-establish stable granulation after filamentous outgrowth: insights from lab-scale experiments. Process. Saf. Environ. Prot. 117, 606–615. https://doi.org/10.1016/j.psep.2018.06.005.
Muñoz-Palazon, B., Pesciaroli, C., Rodriguez-Sanchez, A., Gonzalez-Lopez, J., Gonzalez-Martinez, A., 2018. Pollutants degradation performance and microbial community structure of aerobic granular sludge systems using inoculums adapted at mild and low temperature. Chemosphere 204, 431–441. https://doi.org/10.1016/j.chemosphere.2018.04.062.
Muñoz-Palazon, B., Rodriguez-Sanchez, A., Hurtado-Martinez, M., Gonzalez-Lopez, J., Pfetzing, P., Gonzalez-Martinez, A., 2020a. Performance and microbial community structure of aerobic granular bioreactors at different operational temperature. J. Water Process Eng. 33, 101110 https://doi.org/10.1016/j.jwpe.2019.101110.
Muñoz-Palazon, B., Rodriguez-Sanchez, A., Hurtado-Martinez, M., Santana, F., Gonzalez-Lopez, J., Mack, L., Gonzalez-Martinez, A., 2020b. Polar Arctic Circle biomass enhances performance and stability of aerobic granular sludge systems operated under different temperatures. Bioresour. Technol. 300, 122650 https://doi.org/10.1016/j.biortech.2019.122650.
Muñoz-Palazon, B., Rosa-Masegosa, A., Vilchez-Vargas, R., Link, A., Gorrasi, S., Gonzalez-Lopez, J., Gonzalez-Martinez, A., 2022. Biological removal processes in aerobic granular sludge for treating synthetic hospital wastewater: effect of temperature. J. Water Process Eng. 47, 102691 https://doi.org/10.1016/j.jwpe.2022.102691.
Poretsky, R., Rodriguez-R, L.M., Luo, C., Tsementzi, D., Konstantinidis, K.T., 2014. Strengths and limitations of 16S rRNA gene amplicon sequencing in revealing temporal microbial community dynamics. PLoS One 9 (4), 93827. https://doi.org/10.1371/journal.pone.0093827.
Pronk, M., de Kreuk, M.K., de Bruin, B., Kamminga, P., Kleerebezem, R., van Loosdrecht, M.C.M., 2015. Full scale performance of the aerobic granular sludge process for sewage treatment. Water Res. 84, 207–217. https://doi.org/10.1016/j.watres.2015.07.011.
Regmi, P., Thomas, W., Schafran, G., Bott, C., Rutherford, B., Waltrip, D., 2011. Nitrogen removal assessment through nitrification rates and media biofilm accumulation in an IFAS process demonstration study. Water Res. 45, 6699–6708. https://doi.org/10.1016/j.watres.2011.10.009.
Rognes, T., Flouri, T., Nichols, B., Quince, C., Mahé, F., 2016. VSEARCH: a versatile open source tool for metagenomics. PeerJ 4, 2584. https://doi.org/10.7717/peerj.2584.

Shea, K., Chesson, P., 2002. Community ecology theory as a framework for biological invasions. Trends Ecol. Evol. 17 (4), 170–176. https://doi.org/10.1016/S0169-5347(02)02495-3.

Spieck, E., Wegen, S., Keuter, S., 2021. Relevance of Candidatus Nitrotoga for nitrite oxidation in technical nitrogen removal systems. Appl. Microbiol. Biotechnol. 105 (19), 7123–7139. https://doi.org/10.1007/s00253-021-11487-5.

Stokholm-Bjerregaard, M., McIlroy, S.J., Nierychlo, M., Karst, S.M., Albertsen, M., Nielsen, P.H., 2017. A critical assessment of the microorganisms proposed to be important to enhanced biological phosphorus removal in full-scale wastewater treatment systems. Front. Microbiol. 8, 718. https://doi.org/10.3389/fmicb.2017.00718.

Strubbe, L., van Dijk, E.J.H., Deenekamp, P.J.M., van Loosdrecht, M.C.M., Volcke, E.I., 2023. Oxygen transfer efficiency in an aerobic granular sludge reactor: Dynamics and influencing factors of alpha. Chem. Eng. J. 452, 139548 https://doi.org/10.1016/j.cej.2022.139548.

Toja Ortega, S., Pronk, M., de Kreuk, M.K., 2021a. Anaerobic hydrolysis of complex substrates in full-scale aerobic granular sludge: enzymatic activity determined in different sludge fractions. Appl. Microbiol. Biotechnol. 105 (14), 6073–6086. https://doi.org/10.1007/s00253-021-11443-3.

Toja Ortega, S., Pronk, M., de Kreuk, M.K., 2021b. Effect of an increased particulate COD load on the aerobic granular sludge process: a full scale study. Processes 9 (8), 1472. https://doi.org/10.3390/pr9081472.

Wang, S., Li, Z., Wang, D., Li, Y., Sun, L., 2020. Performance and population structure of two carbon sources granular enhanced biological phosphorus removal systems at low temperature. Bioresour. Technol. 300, 122683 https://doi.org/10.1016/j.biortech.2019.122683.

Wang, W., Yan, Y., Song, C., Pan, M., Wang, Y., 2018. The microbial community structure change of an anaerobic ammonia oxidation reactor in response to decreasing temperatures. Environ. Sci. Pollut. Res. 25 (35), 35330–35341. https://doi.org/10.1007/s11356-018-3449-1.

Watts, S.C., Ritchie, S.C., Inouye, M., Holt, K.E., 2018. FastSpar: rapid and scalable correlation estimation for compositional data. Bioinformatics 35 (6), 1064–1066. https://doi.org/10.1093/bioinformatics/bty734.

Weissbrodt, D.G., Schneiter, G.S., Fürbringer, J.-M., Holliger, C., 2013. Identification of trigger factors selecting for polyphosphate- and glycogen-accumulating organisms in aerobic granular sludge sequencing batch reactors. Water Res. 47 (19), 7006–7018. https://doi.org/10.1016/j.watres.2013.08.043.

Winkler, M.-K., Bassin, J., Kleerebezem, R., van der Lans, R., van Loosdrecht, M., 2012. Temperature and salt effects on settling velocity in granular sludge technology. Water Res. 46 (16), 5445–5451. https://doi.org/10.1016/j.watres.2012.07.022.

Winkler, et al., 2011. Selective sludge removal in a segregated aerobic granular biomass system as a strategy to control PAO-GAO competition at high temperatures. Water Res. 45 (11), 3291–3299. https://doi.org/10.1016/j.watres.2011.03.024.

Yan, X., Zheng, S., Yang, J., Ma, J., Han, Y., Feng, J., Su, X., Sun, J., 2020. Effects of hydradynamic shear stress on sludge properties, N_2O generation, and microbial community structure during activated sludge process. J. Environ. Manag. 274, 111215 https://doi.org/10.1016/j.envman.2020.111215.

Yuan, H., Li, Y., Zhang, X., Wang, X., Wang, H., 2019. Alteration of denitrifying microbial communities by redox mediators available at low temperature. Water Sci. Technol. 79 (7), 1253–1262. https://doi.org/10.2166/wst.2019.116.

Zhou, H., Li, X., Xu, G., Yu, H., 2018. Overview of strategies for enhanced treatment of municipal/domestic wastewater at low temperature. Sci. Total Environ. 643, 225–237. https://doi.org/10.1016/j.scitotenv.2018.06.100.